Plant Cell Physiol. 40(11): 1134–1142 (1999)
JSPP © 1999

Identification and Characterization of *Arabidopsis* Mutants with Reduced Quenching of Chlorophyll Fluorescence

Toshiharu Shikanai [1, 3], Yuri Munekage [1], Katsumi Shimizu [1], Tsuyoshi Endo [2] and Takashi Hashimoto [1]

[1] *Graduate School of Biological Sciences, Nara Institute of Science and Technology, Ikoma, Nara, 630-0101 Japan*
[2] *Division of Integrated Life Science, Graduate School of Biostudies, Kyoto University, Sakyoku, Kyoto, 606-8502 Japan*

Regulation of nonradiative dissipation of absorbed light energy in PSII is an indispensable process to avoid photoinhibition in plants. To dissect molecular mechanisms of the regulation, we identified *Arabidopsis* mutants with reduced quenching of Chl fluorescence using a fluorescence imaging system. By analyses of Chl fluorescence induction pattern in the light and quantum yield of both photosystems, 37 mutants were classified into three groups. The first group was characterized by an extremely high level of minimum Chl fluorescence at the open PSII center possibly due to a defect in PSII. Mutants with significant reduction in the nonphotochemical quenching formation but not in quantum yield of both photosystems were classified into the second group. Mutants in the third group showed reduction in quantum yield of both photosystems possibly due to a defect in the electron transport activity. Mutants in the second and third groups were further characterized by light intensity dependence of Chl fluorescence parameters and steady state redox level of P700.

Key words: *Arabidopsis thaliana* — Chlorophyll fluorescence — Electron transport — Mutant — Nonphotochemical quenching — Photosynthesis.

Chl *a* fluorescence emitted from PSII reflects the state of photosynthetic electron transport. Since limitation of electron transport leading to reduction of the primary quinone-type acceptor Q_A increases the fluorescence level, monitoring of Chl fluorescence has been utilized to identify mutants lacking photosynthetic activities (Miles 1980, Barkan et al. 1986). Most of the high-Chl fluorescence mutants are defective in components of the main pathway of photosynthetic electron transport and are often seedling-lethal under photoautotrophic growth conditions (Meurer et al. 1996, Dinkins et al. 1997).

Recent improvements of fluorescence measuring techniques including the introduction of a pulse amplitude modulation (PAM) fluorescence system have facilitated more precise interpretation of the fluorescence signals. It is now generally accepted that Chl fluorescence reflects the regulation of absorbed light energy dissipation in a complex manner, as well as utilization of the light energy (Krause and Weis 1991). This idea was successfully introduced into mutant identification concerning the regulatory mechanisms of light harvesting in PSII using *Chlamydomonas reinhardtii* (Niyogi et al. 1997a, b) and *Arabidopsis thaliana* (Niyogi et al. 1998, Pogson et al. 1998, Havaux and Niyogi 1999). In these studies, Niyogi et al. developed a fluorescence imaging system using a charge-coupled device (CCD) camera, which made it possible to identify a mutant with subtle alteration in Chl fluorescence quenching.

Since the absorption of light energy often exceeds the capacity of utilization, regulation of light harvesting is an indispensable process in plants to avoid damage to the photosynthetic apparatus (photoinhibition) (Demmig-Adams and Adams III 1992, Horton et al. 1996, Niyogi 1999). The extent of nonradiative dissipation of absorbed light energy can be estimated from the extent of nonphotochemical quenching (NPQ) of Chl fluorescence (Krause and Weis 1991). NPQ arises from several processes sensing the level of excessive light intensity and transducing it to the light harvesting system. NPQ due to the state transition (qT) is induced by monitoring the redox state of plastoquinone (Fork and Satoh 1986, Zito et al. 1999). In higher plants, however, qT is small and is unlikely to contribute to photoprotection. Under light stress conditions, irreversible or slowly reversible quenching including the photodamage of PSII reaction center also contributes to NPQ (qI). The major factor of NPQ, however, depends on the trans-thylakoid membrane pH gradient (ΔpH) and is called energy-dependent quenching (qE). Lumen acidity serves at least two roles in the NPQ formation. First, it activates the conversion of xanthophyll carotenoids which play an important role in generating qE (Demmig et al. 1987, Demmig-Adams et al. 1989). Under excess light, violaxanthin is converted rapidly to zeaxanthin via the intermediate antheraxanthin, and this reaction is reversed under a low light intensity (xanthophyll cycle). The level of zeaxanthin and antheraxanthin is correlated with the extent of qE (Dem-

Abbreviations: ΔpH, trans-thylakoid membrane pH gradient; Fm, maximum Chl fluorescence at the closed PSII center in the dark-adapted plants; Fm', maximum Chl fluorescence at the closed PSII center in the light; Fo, minimum Chl fluorescence at the open PSII center in the dark; Fs, steady state Chl fluorescence in the light; Fv, variable Chl fluorescence (Fm–Fo); NPQ, nonphotochemical quenching.

[3] To whom correspondence should be addressed. Fax, +81-743-72-5489; E-mail, shikanai@bs.aist-nara.ac.jp

Downloaded from https://academic.oup.com/pcp/article/40/11/1134/1880967 by U.S. Department of Justice user on 16 August 2022

mig-Adams and Adams III 1996). Second, lumen acidity also induces protonation of the Chl *a/b* binding proteins of light harvesting complex II, resulting in conformational changes that are necessary for the NPQ formation (Bilger and Björkman 1990, 1994, Noctor et al. 1993, Ruban et al. 1993). In spite of extensive biochemical and physiological studies, the molecular mechanisms to dissipate excess light energy from PSII are still a matter of discussion.

Since the qE formation depends on ΔpH, the formation of ΔpH should be precisely regulated to cope with changes in ambient light conditions. The extent of the linear electron transport from H_2O to $NADP^+$, however, is influenced by many physiological and environmental factors, including light intensity, extent of CO_2 uptake from stomata and nutrient conditions. Auxiliary electron flows, water-water cycle and cyclic electron flow around PSI, promote the NPQ formation (Heber and Walker 1992, Fork and Herbert 1993, Bendall and Manasse 1995, Asada 1999, Endo et al. 1999). Photorespiration also contributes to maintain ΔpH especially under stress conditions such as drought, in which electron acceptor $NADP^+$ is limited by a decrease in CO_2 fixation rate (Kozaki and Takeba 1996). When mutations on the auxiliary electron transport pathways lead to significant alteration in Chl fluorescence quenching, mutants can be identified by the Chl fluorescence imaging system. As a step to advance our understanding of the regulatory mechanisms of light harvesting in PSII, we have identified *Arabidopsis* mutants with reduced quenching of Chl fluorescence.

Materials and Methods

Plant materials and growth conditions—*Arabidopsis thaliana* M_2 seeds (ecotypes Columbia *gl1* and Landsberg *erecta*) mutagenized by ethyl methanesulfonate (EMS) were obtained from Lehle Seeds (Round Rock, TX). Seedlings were cultured in soil in a culture room (50 μmol m^{-2} s^{-1}, 16 h-light/8 h-dark cycles at 23°C) for 2 weeks. Prior to screening, seedlings were dark-adapted at least for 10 min. Mutants isolated were characterized using an M_3 generation grown in a greenhouse in Fig. 2–5 and Table 2. In Fig. 6, plants grown in a culture room were used.

Mutant screening—Mutant screening was performed by using an imaging system of Chl fluorescence (Niyogi et al. 1997a) with some modifications. Chl fluorescence of dark-adapted leaves (F) was monitored immediately after the exposure to activating light (200 μmol m^{-2} s^{-1}). The light source was equipped with a filter transmitting light in the spectral range less than 590 nm. Actinic light at an intensity high enough to induce NPQ (300 μmol m^{-2} s^{-1}) was supplied from the activating light source without using the filter. After the exposure to the actinic light for 2 min, Chl fluorescence image was recorded again (F′). The extent of quenching was determined by comparing two fluorescence images, F and F′. The fluorescence image was recorded by a CCD camera (C5985, Hamamatsu Photonics, Japan) equipped with a filter transmitting light longer than 680 nm.

Analysis of Chl fluorescence induction—Chl fluorescence was measured with a PAM Chl fluorometer (Walz, Effeltrich, Germany), with an emitter-detector unit ED101. The minimum Chl fluorescence at the open PSII center (Fo), was determined by measuring light (650 nm) at a light intensity of 0.05–0.1 μmol m^{-2} s^{-1}. A saturating pulse of white light (800 ms, 3,000 μmol m^{-2} s^{-1}) was applied to determine Fm and the ratio Fv/Fm = (Fm − Fo)/Fm. Actinic white light (50–2,100 μmol m^{-2} s^{-1}) was applied to determine the quantum yield of PSII $\{\Phi_{PSII} = (Fm' - Fs)/Fm'\}$, where Fm′ is the maximum Chl fluorescence at the closed PSII center in the light, and Fs is the steady state Chl fluorescence in the light (Genty et al. 1989). Fs was recorded after 4 min of actinic light irradiation. To determine the extent of NPQ $\{(Fm - Fm')/Fm'\}$, actinic light was applied at a light intensity of 50–2,100 μmol m^{-2} s^{-1}. Reduction levels of Q_A $(1 - q_P)$ were calculated by the equation $\{1 - (Fm' - Fs)/(Fm' - Fo')\}$, where Fo′ is the minimal steady-state fluorescence level of light-adapted leaves.

Measurement of redox changes in P700—Redox changes of P700 were analyzed with a PAM Chl fluorometer with an emitter-detector unit ED 800T (Schreiber et al. 1988). The quantum yield of PSI $(\Phi_{PSI} = 1 - \Delta A/\Delta A_{FR})$ was estimated by monitoring the light-induced absorbance change of P700 at 839 nm (Harbinson and Woodward 1987). The in vivo absorbance change of P700 (ΔA) was recorded immediately after interruption of the actinic light (50 μmol m^{-2} s^{-1}). ΔA_{FR} is the in vivo absorbance change of P700 by far-red light (720 nm, 0.66 μmol m^{-2} s^{-1}). Since P700 pool was not fully oxidized by the far-red light used, ΔA_{FR} was lower than the maximum in vivo absorbance change of P700 (ΔA_{max}). The steady state redox level of P700 ($\Delta A/\Delta A_{FR}$) was also analyzed at actinic light intensities of 100–1,000 μmol m^{-2} s^{-1}.

Results

Screening of mutants with reduced quenching of Chl fluorescence—*Arabidopsis* mutants with reduced Chl fluorescence were identified using a Chl fluorescence imaging system. Seedlings from seeds mutagenized by EMS were cultured in soil to eliminate seedling lethal mutants under photoautotrophic conditions. Seedlings were maintained at a low light intensity (50 μmol m^{-2} s^{-1}) in order to recover mutants that might be sensitive to high intensity light. Chl fluorescence images were recorded before turning on and just after turning off the actinic light (300 μmol m^{-2} s^{-1} for 2 min). As shown in Fig. 1, Chl fluorescence decreased during the actinic light irradiation due to both dissipation (NPQ) and utilization (photochemical quenching) of absorbed light energy. Quenching of Chl fluorescence was calculated from the fluorescence images using the equation, F-F′, where F is the fluorescence image captured before onset of the actinic light (Fig. 1A), and F′ is that just after the actinic light irradiation (Fig. 1B). Seedlings with lesser quenching of Chl fluorescence were selected as putative mutants.

As a second screening, Chl fluorescence induction patterns were further characterized by PAM Chl fluorometry using two different actinic light intensities (100 and 370 μmol m^{-2} s^{-1}). We screened approximately 21,000 M_2 seeds (13,000 seeds of ecotype Landsberg *erecta* and 8,000 seeds of ecotype Columbia *gl1*) and identified 37 mutants. Mutants showed divergent visible phenotypes including changes in color of leaves and growth rate (Table

Downloaded from https://academic.oup.com/pcp/article/40/11/1134/1880967 by U.S. Department of Justice user on 16 August 2022

Table 1 General feature and F_2 segregation analysis of mutants

Line[a]	Segregation data[b]			Growth rate[d]	Visible phenotypes
	F_1	F_2	χ^2[c]		
group 1					
LE16-7	nd[e]			+	
LE16-10	nd[e]			+	
LE17-3	0/4	10/42	0.03	++	
LE17-4	0/3	13/67	1.12	++	
LE18-28	0/4	7/51	3.46	++	
LE18-30	nd[e]			+	
CE10-6-3	nd[e]			+	
CE10-9-4	0/5	11/46	0.03	++	
CE10-4	nd[e]			++	
CE12-4-1	0/1	14/66	0.51	+++	
group 2					
LE16-1	0/3	8/35	0.09	+++	
LE20-7-1	0/4	nd[f]		+++	
LE20-14	0/4	4/25	1.08	+++	
CE10-10-1	0/2[g]	18/70	0.06	+++	
CE10-12-2	0/4	nd[f]		+++	
CE10-15-3	nd[e]			+	wilted
CE11-8-1	0/4	12/61	0.82	+++	
CE12-13	0/4	15/68	0.31	+++	
group 3					
LE17-8	0/1	23/143	7.06	++	
LE17-11	0/4	23/102	0.35	++	
LE18-10	nd[e]			+	
LE18-18	nd[e]			+	
LE18-24	nd[e]			+	
LE18-27	nd[e]			+	
CE10-5-3	0/4	17/86	1.26	++	
CE10-10-2	0/3	9/39	0.07	++	
CE10-11-4	0/1	18/73	0.00	++	
CE11-1-1	0/5	17/79	0.41	+++	
CE11-3-1[h]	nd			+	pale green
CE11-3-2[h]	nd			+	pale green
CE11-4[h]	0/3	14/62	0.19	+	pale green
CE11-5[h]	nd			+	pale green
CE11-6[h]	nd			+	pale green
CE11-8-2[h]	nd			+	pale green
CE11-10[h]	nd			+	pale green
CE11-12-2[h]	nd			+	pale green
CE12-10	0/4	12/51	0.06	++	

[a] Background of mutants with code name LE and CE are Landsberg *erecta* and Columbia *gl1*, respectively.
[b] represented by (number of seedlings exhibiting mutant phenotypes)/(total number of seedlings).
[c] χ^2 values were calculated for an expected segregation in F_2 progenies of one mutant to three wild types.
[d] +++, similar to the wild type; ++, reduced; +, severely reduced.
[e] F_1 progeny could not be obtained due to the severely reduced growth rate.
[f] Mutant phenotype was so subtle that it cannot be identified as individuals in F_2 generation.
[g] F_1 progeny showed slightly reduced NPQ, indicating the semidominant nature of mutation.
[h] These lines are allelic to one another.

Downloaded from https://academic.oup.com/pcp/article/40/11/1134/1880967 by U.S. Department of Justice user on 16 August 2022

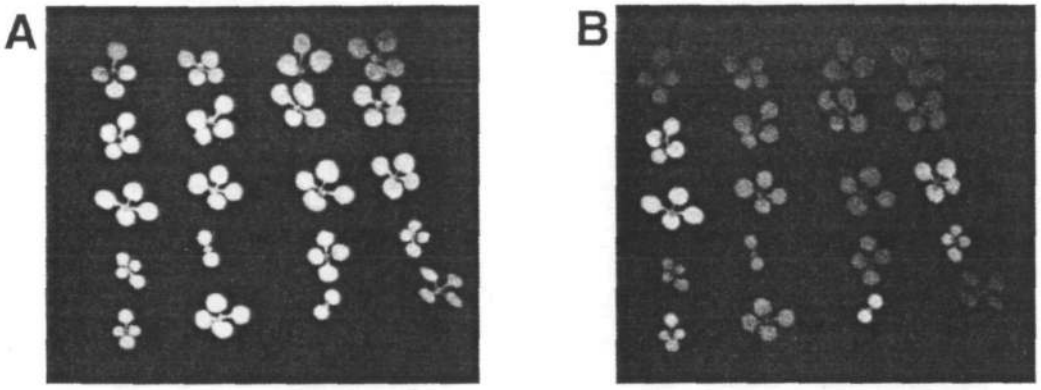

Fig. 1 Imaging of Chl fluorescence quenching. Chl fluorescence images of F_2 progenies (CE10-10-1 × wild type, ecotype Columbia *gl1*) were captured before (A) and just after (B) actinic light irradiation (300 μmol m^{-2} s^{-1} for 2 min).

1). Genetic segregation analysis confirmed the recessive nature of the mutations, except for CE10-10-1 which exhibited a semidominant nature (Table 1). Slight deviation from the expected 25% for a single recessive mutant was observed in LE18-28 and CE17-8, which may be explained by selection due to the reduced growth rate. Due to the severely reduced growth rate in 10 lines, F_1 seeds were not obtained (Table 1). F_2 segregation was not scored in LE20-7-1 and CE10-12-2, since alteration in Chl fluorescence was so subtle that mutant phenotypes could not be identified as individuals in the F_2 generation. Inheritance of mutant phenotypes was confirmed in the M_3 generation in these lines (data not shown). Crossings between mutants with similar Chl fluorescence parameters showed that CE11-3-1, CE11-3-2, CE11-4, CE11-5, CE11-6, CE11-8-2, CE11-10 and CE11-12-2 had a defect on the same locus.

Mutant classification based on Chl fluorescence induction patterns—According to the patterns obtained by PAM Chl fluorometry, the mutants were classified into at least three groups. Ten mutants were classified into the first group, which is characterized by extremely high Fo. Fig. 2 shows the Chl fluorescence patterns of LE17-4 as a representative of this group, as well as those of the wild type. Fv/Fm is very low (0.52) due to high Fo in LE17-4. The fluorescence level dropped below Fo at 1,000 μmol m^{-2} s^{-1}. This phenomenon depended on light intensity and was not evident at a low light intensity (50 μmol m^{-2} s^{-1}). Consequently, Fs was lower at a higher light intensity. The growth rate of mutants was generally low in this group (Table 1). As discussed later, mutants in this group carry some defect in PSII and do not have a direct relationship with the regulation of PSII.

Since the NPQ formation was tightly correlated with the activity of the photosynthetic electron transport, reduction in NPQ is caused not only by a direct defect in the machinery concerning the NPQ formation (NPQ mutant) but also by that in the electron transport pathways (electron transport mutant). Since NPQ functions to dissipate excessive absorbed light energy, the NPQ mutant should show rather normal fluorescence characters at a low light intensity, where photochemical quenching is predominant. We selected group 2 mutants as candidates of NPQ mutants under the following criteria; (1) minor effect on quantum yield of both photosystems at a low light intensity, (2) minor effect on Fv/Fm values under the greenhouse culture conditions, and (3) normal growth rate under the greenhouse culture conditions.

Table 2 summarizes the quantum yield of both photosystems. As a representative of NPQ mutant, *npq1-2*, which lacks the violaxanthin deepoxidase gene, was also analyzed (Niyogi et al. 1998). Eight mutants were classified

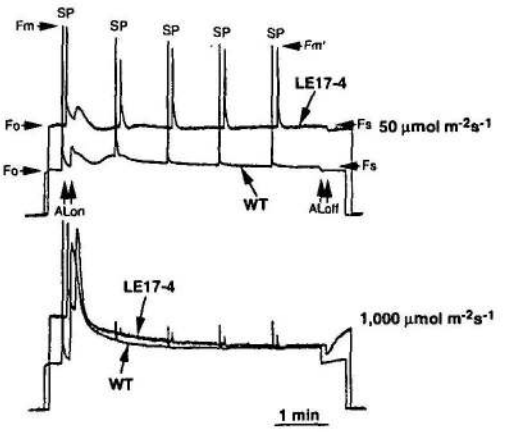

Fig. 2 Comparison of the Chl fluorescence induction patterns between LE17-4 and the wild type (WT, ecotype Landsberg *erecta*). Chl fluorescence was induced by actinic light (AL) irradiation (50 μmol m^{-2} s^{-1} and 1,000 μmol m^{-2} s^{-1} for 5 min). Saturating pulses (SP) were applied every 1 min to measure Fm and Fm'.

Downloaded from https://academic.oup.com/pcp/article/40/11/1134/1880967 by U.S. Department of Justice user on 16 August 2022

Table 2 Parameters of the Chl fluorescence and the redox kinetics of P700

	Φ_{PSII} [a]	Φ_{PSI} [a]	NPQ [b]	Fv/Fm
wild type				
Landsberg *erecta*	0.67	0.97	1.24	0.75
Columbia *gl1*	0.71	0.95	1.10	0.76
group 2				
npq1-2	0.67	0.93	0.40	0.72
LE16-1	0.64	0.94	0.82	0.73
LE20-7-1	0.67	0.95	0.98	0.74
LE20-14	0.62	0.94	0.64	0.68
CE10-10-1	0.61	0.89	0.12	0.71
CE10-12-2	0.62	0.91	0.88	0.73
CE10-15-3	0.63	0.94	0.69	0.74
CE11-8-1	0.65	0.95	1.00	0.73
CE12-13	0.63	0.96	0.40	0.74
group 3				
LE17-8	0.54	0.88	0.47	0.66
LE17-11	0.63	0.81	0.67	0.70
LE18-10	0.53	0.86	0.86	0.66
LE18-18	0.67	0.67	1.09	0.56
LE18-24	0.58	0.90	0.76	0.62
LE18-27	0.60	0.89	0.85	0.68
CE10-5-3	0.52	0.57	0.09	0.62
CE10-10-2	0.56	0.78	0.63	0.68
CE10-11-4	0.25	0.59	0.63	0.48
CE11-1-1	0.60	0.97	0.53	0.70
CE11-4	0.51	0.84	0.61	0.64
CE12-10	0.56	0.95	0.29	0.65

[a] Quantum yield of PSI (Φ_{PSI}) and PSII (Φ_{PSII}) was determined at 50 μmol m^{-2} s^{-1}.
[b] NPQ was determined at 1,000 μmol m^{-2} s^{-1}.

into the second group, which is characterized by a rather normal quantum yield of PSI (more than 0.89) and PSII (more than 0.61). Fv/Fm is only slightly affected (0.68–0.74). *npq1-2* is classified into this group. In contrast, mutants with a reduced quantum yield of PSI (less than 0.88) or PSII (less than 0.6) were classified into the third group. Fv/Fm is also low (0.48–0.7) under the greenhouse culture conditions in this group. Although the boundary is not distinctive in quantum yield of the two photosystems between group 2 and group 3 mutants (compare CE10-10-1 with LE18-27 in Table 2), comparison of the growth rate allowed us to classify the mutants. While group 2 mutants grew as vigorously as the wild type, the growth rate of group 3 mutants was significantly reduced (Table 1). Exceptions are CE10-15-3 that has a wilted phenotype and CE11-1-1. Considering the criteria of classification, mutants with a subtle defect in the electron transport activity may be classified into the second group, as well as NPQ mutants. On the contrary, mutants with significant reduc-

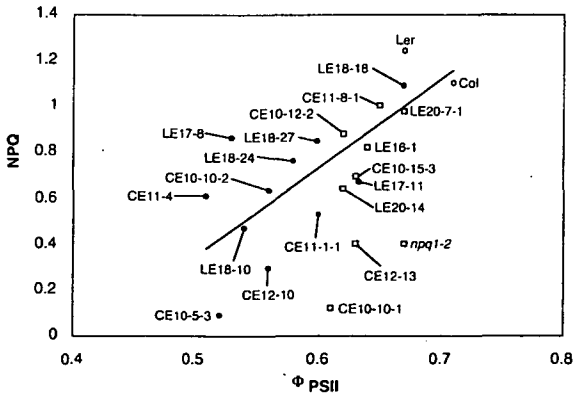

Fig. 3 Two-dimensional plots of quantum yield of PSII (Φ_{PSII}) and NPQ. Open circles (wild types) and closed circles (group 3 mutants) were fit by linear regression ($r^2=0.56$). Open squares indicate plots of group 2 mutants. CE10-11-4 is plotted out of the field.

Downloaded from https://academic.oup.com/pcp/article/40/11/1134/1880967 by U.S. Department of Justice user on 16 August 2022

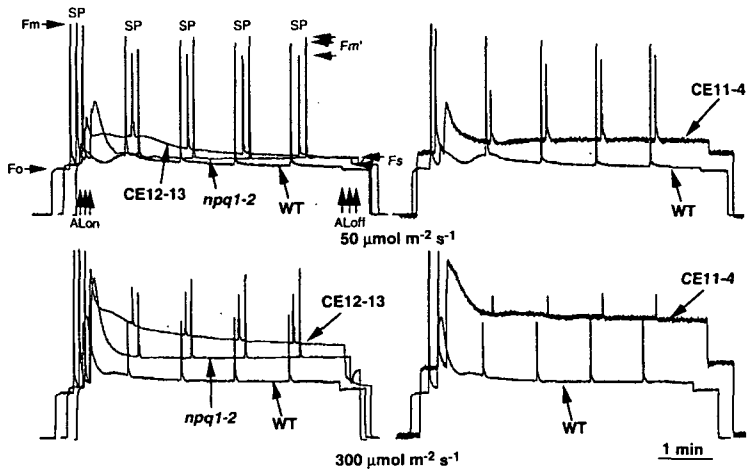

Fig. 4 Comparison of the Chl fluorescence induction patterns among CE12-13, *npq1-2*, CE11-4 and the wild type (WT, ecotype Columbia *gl1*). Chl fluorescence was induced by actinic light (AL) irradiation (50 μmol m^{-2} s^{-1} and 300 μmol m^{-2} s^{-1} for 5 min). Saturating pulses (SP) were applied every 1 min to measure Fm and Fm'.

tion in the electron transport activity should be classified into the third group.

Figure 3 shows the two-dimensional plots of quantum yield of PSII and NPQ in the group 2 and 3 mutants. Since NPQ formation depends on the electron transport activity, NPQ and quantum yield of PSII should be correlated in the wild type and electron transport mutants, in which retarded electron transport activity leads to a reduction in NPQ. In Fig. 3, NPQ and quantum yield of PSII were fitted by linear regression in the wild type and group 3 mutants. When there is a defect directly in the machinery concerning the NPQ formation, reduction in NPQ is not directly correlated with the electron transport activity and plots should deviate from this linear regression. Two mutants, CE10-10-1 and CE12-13 showed a significant deviation as well as *npq1-2*, suggesting that the defect concerns the NPQ formation in these mutants.

Characterization of representative mutants—Figure 4 shows the Chl fluorescence patterns of CE12-13 representing a group 2 mutant, CE11-4 representing a group 3 mutant, *npq1-2* and the wild type. At a low light intensity (50 μmol m^{-2} s^{-1}), NPQ was only slightly affected in all mutants. Although the Fs level was significantly high in CE11-4, it was rather normal in CE12-13 and *npq1-2*. At a higher light intensity (300 μmol m^{-2} s^{-1}), however, lower NPQ and higher Fs was evident in all mutants. Although NPQ was similar in CE12-13 and CE11-4 at both light intensities, the Fs level was much higher in CE11-4 than in CE12-13, which is expressed as a decrease in quantum yield of PSII in the light (Fig. 5).

Figure 5 shows the light-response curves of Chl fluorescence parameters, NPQ and quantum yield of PSII (Φ_{PSII}) among CE12-13, CE11-4 and the wild type. At a high light intensity, CE11-4 exhibited a much lower steady state NPQ and quantum yield of PSII than did the wild type. Electron carriers were saturated by electrons at 2,100

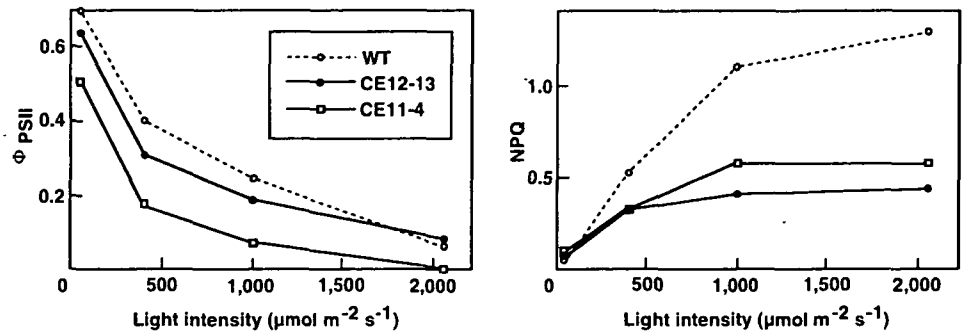

Fig. 5 Light intensity dependence of steady state Chl fluorescence parameters, quantum yield of PSII photochemistry in the light (Φ_{PSII}) (A) and NPQ (B) in CE12-13, CE11-4 and the wild type (ecotype Columbia *gl1*).

Downloaded from https://academic.oup.com/pcp/article/40/11/1134/1880967 by U.S. Department of Justice user on 16 August 2022

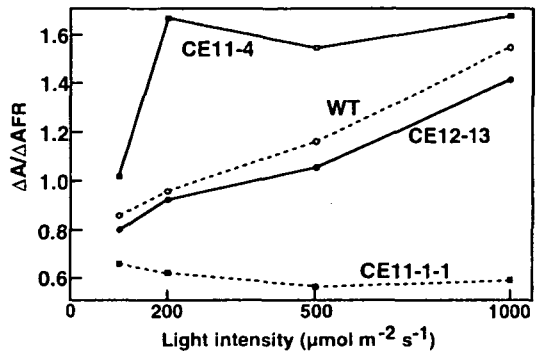

Fig. 6 Light intensity dependence of steady state redox level of P700 ($\Delta A/\Delta A_{FR}$) in CE12-13, CE11-4, CE11-1-1 and the wild type (WT, ecotype Columbia *gl1*). Redox state of P700 was monitored after actinic light irradiation (100–1,000 μmol m^{-2} s^{-1}) for 2 min.

μmol m^{-2} s^{-1} in CE11-4, as judged from the very low photochemical quenching. Although the extent of NPQ was similar in CE12-13 and CE11-4 at a light intensity lower than 500 μmol m^{-2} s^{-1}, Φ_{PSII} was higher in CE12-13 than in CE11-4. The low quantum yield of PSII in CE11-4 was due to a high level of Fs (Fig. 4), indicating that reduction in the electron transport activity on the reducing side of plastoquinone resulted in a higher reduction level of plastoquinone pool in the light. On the other hand, Φ_{PSII} of CE12-13 was similar to that of the wild type at higher light intensities (1,000–2,100 μmol m^{-2} s^{-1}), and electron carriers were not saturated by electrons. Reduction levels of Q_A ($1-q_P$) at 300 μmol m^{-2} s^{-1} were 0.08 (wild type), 0.31 (CE12-13) and 0.68 (CE11-4).

A subtle defect in the electron transport pathways may exhibit similar phenotypes with the NPQ mutant in quantum yield of both photosystems at a low light intensity. To characterize mutations more precisely, we analyzed the steady state redox level of P700 at an actinic light intensity of 100–1,000 μmol m^{-2} s^{-1}. Fig. 6 shows the results in CE12-13, CE11-4 and CE11-1-1, as well as the wild type. Since the P700 pool was not fully oxidized by the far-red light used (see Materials and Methods), ΔA often exceeded ΔA_{FR}. In CE11-4, the oxidation level of P700 was very high. The primary defect appears to be located in the intersystem electron transport pathways. In contrast, the steady-state level of P700 oxidation was very low in CE11-1-1. CE11-1-1 appears to have a defect in PSI or in electron acceptors from PSI. CE12-13 showing typical characters of NPQ mutants (Fig. 3–5) was also analyzed. Although reduction in NPQ leads to the overloading of electrons in the intersystem theoretically, the steady-state level of P700 oxidation was similar to that of the wild type in CE12-13.

Discussion

We have identified 37 mutants exhibiting reduced Chl fluorescence quenching, indicating that 0.2% of M_2 seedlings exhibited mutant phenotypes. Considering differences in phenotypes and results of complementation tests among mutants, each mutation is likely to be on a different locus. The only exception was that CE11-4 was allelic to seven other mutants which originated from the same M_1 seed pool. The results suggest that mutations on many loci lead to a similar phenotype, reduction in Chl fluorescence quenching, and our screening was not saturated. Actually, the 37 mutants do not include a mutant allelic to *npq1* (Niyogi et al. 1998).

Meurer et al. also identified 34 high-Chl-fluorescence (*hcf*) mutants (Meurer et al. 1996). In their screening system, seedlings were placed in the dark for 15 min and then irradiated UV light (3,400 mW cm^{-2}) indicating that Chl florescence quenching should be mainly photochemical. This is supported by the fact that 22 mutants were seedling-lethal possibly due to the complete loss of photosynthetic electron transport activity. In contrast, we have identified mutants with reduced quenching of Chl fluorescence in the light (300 μmol m^{-2} s^{-1}). Under this screening conditions, NPQ contributes more than photochemical quenching. Furthermore, seedling-lethal mutants were eliminated by culturing seedlings in soil. Therefore, the mutant population of our 37 mutants should be quite different from that of the *hcf* mutants previously isolated (Meurer et al. 1996).

The 34 *hcf* mutants were classified into six groups by analyses of the Chl fluorescence induction patterns and the redox kinetics of P700 (Meurer et al. 1996). To estimate the defective points, we also applied similar analyses to our mutants. According to the mutant classification by Meurer et al. (Meurer et al. 1996), our group 1 mutants correspond to their group III mutants having defects in PSII. Western analysis showed a reduced level of PSII subunits in their group III mutants (Meurer et al. 1996). We also found that one of the mutants in this group, LE18-30, accumulated a slightly smaller version of 33 kDa proteins in the oxygen evolving complex than those of wild type by Western analysis (data not shown). A similar fluorescence pattern was also observed in PSII particles treated with Tris to release the oxygen evolving complex (Schreiber and Neubauer 1987). Mutants in this group are easily identified by (1) the significant reduction in Fv/Fm and (2) enhanced quenching below Fo at a high light intensity. However, the possibility that the primary defect is not in PSII cannot be ruled out, since similar fluorescence kinetics are observed in plants suffering photoinhibition.

According to the quantum yield of both photosystems, group 2 and group 3 mutants were distinguished from each other. Considering the significant reduction in

Downloaded from https://academic.oup.com/pcp/article/40/11/1134/1880967 by U.S. Department of Justice user on 16 August 2022

quantum yield of both photosystems and retarded growth, mutants with an intensive defect in the electron transport pathways must be classified into the third group. On the other hand, the quantum yield of both photosystems was only slightly affected in group 2 mutants. When the defect is in the machinery concerning the NPQ formation, electron transport activity should be only slightly affected at a low light intensity, where photochemical quenching is predominant. This hypothesis was confirmed by the fact that *npq1-2* was classified into group 2. HPLC analysis of carotenoid compositions showed that xanthophyll cycle activity was significantly reduced in CE10-10-1 (unpublished data), suggesting that the mutant has a defect in the machinery concerning the NPQ formation.

A subtle defect in the electron transport activity should lead to a phenotype similar to that of the NPQ mutant, minor effect on quantum yield of both photosystems. Group 2 may contain electron transport mutants with a subtle defect, which are difficult to distinguish from NPQ mutants with a subtle defect. However, a mutant with a significant defect in the machinery of NPQ formation can be identified by the deviation from the linear regression of NPQ and quantum yield of PSII (CE10-10-1 and CE12-3 in Fig. 4).

We thank Dr. Krishna K. Niyogi for his gift of *npq1-2* seeds and critical reading of the manuscript. We also thank Dr. Arthur R. Grossman for his advice in constructing the screening system, and Momoko Miyata for her help in mutant screening. This work was supported by a Research for the Future Program (Multiple molecular improvement of photosynthesis and plant performances for crop productivity, JSPS-RFTF97R16001) from the Japan Society for the Promotion of Science.

References

Asada, K. (1999) The water-water cycle in chloroplasts: scavenging of active oxygens and dissipation of excess photons. *Annu. Rev. Plant Physiol. Plant Mol. Biol.* 50: 601–639.

Barkan, A., Miles, D. and Taylor, W.C. (1986) Chloroplast gene expression in nuclear, photosynthetic mutants of maize. *EMBO J.* 5: 1421–1427.

Bendall, D.S. and Manasse, R.S. (1995) Cyclic photophosphorylation and electron transport. *Biochim. Biophys. Acta* 1229: 23–28.

Bilger, W. and Björkman, O. (1990) Role of the xanthophyll cycle in photoprotection elucidated by measurements of light-induced absorbance changes, fluorescence and photosynthesis in leaves of *Hedera canariensis*. *Photosynth. Res.* 25: 173–185.

Bilger, W. and Björkman, O. (1994) Relationships among violaxanthin deepoxidation, thylakoid membrane conformation, and nonphotochemical chlorophyll fluorescence quenching in leaves of cotton (*Gossypium hirsutum* L.). *Planta* 193: 238–246.

Demmig, B., Winter, K., Krüger, A. and Czygan, F.-C. (1987) Photoinhibition and zeaxanthin formation in intact leaves. A possible role of the xanthophyll cycle in the dissipation of excess light energy. *Plant Physiol.* 84: 219–224.

Demmig-Adams, B. and Adams III, W.W. (1992) Photoprotection and other responses of plants to high light stress. *Annu. Rev. Plant Physiol. Plant Mol. Biol.* 43: 599–626.

Demmig-Adams, B. and Adams III, W.W. (1996) Xanthophyll cycle and light stress in nature: uniform response to excess direct sunlight among higher plant species. *Planta* 198: 460–470.

Demmig-Adams, B., Adams III, W.W., Heber, U., Neimanis, S., Winter, K., Krüger, A., Czygan, F.-C., Bilger, W. and Björkman, O. (1989) Inhibition of zeaxanthin formation and of rapid changes in radiationless energy dissipation by dithiothreitol in spinach leaves and chloroplasts. *Plant Physiol.* 92: 293–301.

Dinkins, R.D., Bandaranayake, H., Baeza, L., Griffiths, A.J.F. and Green, B.R. (1997) *hch5*, a nuclear photosynthetic electron transport mutant of *Arabidopsis thaliana* with a pleiotropic effect on chloroplast gene expression. *Plant Physiol.* 113: 1023–1031.

Endo, T., Shikanai, T., Takabayashi, A., Asada, K. and Sato, F. (1999) The role of chloroplastic NAD(P)H dehydrogenase in photoprotection. *FEBS Lett.* 457: 5–8.

Fork, D.C. and Herbert, S.K. (1993) Electron transport and photophosphorylation by photosystem I in vivo in plants and cyanobacteria. *Photosynth. Res.* 36: 149–168.

Fork, D.C. and Satoh, K. (1986) The control by state transitions of the distribution of excitation energy in photosynthesis. *Annu. Rev Plant Physiol.* 37: 335–361.

Genty, B., Briantais, J.-M. and Baker, N.R. (1989) The relationship between the quantum yield of photosynthetic electron transport and quenching of chlorophyll fluorescence. *Biochim. Biophys. Acta* 990: 87–92.

Harbinson, J. and Woodward, F.I. (1987) The use of light-induced absorbance changes at 820 nm to monitor the oxidation state of P700 in leaves. *Plant Cell Environ.* 10: 131–140.

Havaux, M. and Niyogi, K.K. (1999) The violaxanthin cycle protects plants from photooxidative damages by more than one mechanism. *Proc. Natl. Acad. Sci. USA* 96: 8762–8767.

Heber, U. and Walker, D. (1992) Concerning a dual function of coupled cyclic electron transport in leaves. *Plant Physiol.* 100: 1621–1626.

Horton, P., Ruban, A.V. and Walters, R.G. (1996) Regulation of light harvesting in green plants. *Annu. Rev. Plant Physiol. Plant Mol. Biol.* 47: 655–684.

Kozaki, A. and Takeba, G. (1996) Photorespiration protects C3 plants from photooxidation. *Nature* 384: 557–560.

Krause, G.H. and Weis, E. (1991) Chlorophyll fluorescence and photosynthesis: the basics. *Annu. Rev. Plant Physiol. Plant Mol. Biol.* 42: 313–349.

Meurer, J., Meierhoff, K. and Westhoff, P. (1996) Isolation of high-chlorophyll-fluorescence mutants of *Arabidopsis thaliana* and their characterisation by spectroscopy, immunoblotting and Nothern hybridisation. *Planta* 198: 385–396.

Miles, D. (1980) Mutants of higher plants: maize. *Methods Enzymol.* 69: 3–23.

Niyogi, K. (1999) Photoprotection revisited: genetic and molecular approaches. *Annu. Rev. Plant Physiol. Plant Mol. Biol.* 50: 333–359.

Niyogi, K.K., Björkman, O. and Grossman, A.R. (1997a) *Chlamydomonas* xanthophyll cycle mutants identified by video imaging of chlorophyll fluorescence quenching. *Plant Cell* 9: 1369–1380.

Niyogi, K.K., Björkman, O. and Grossman, A.R. (1997b) The roles of specific xanthophylls in photoprotection. *Proc. Natl. Acad. Sci. USA* 94: 14162–14167.

Niyogi, K.K., Grossman, A.R. and Björkman, O. (1998) *Arabidopsis* mutants define a central role for the xanthophyll cycle in the regulation of photosynthetic energy conversion. *Plant Cell* 10: 1121–1134.

Noctor, G., Ruban, A.V. and Horton, P. (1993) Modulation of ΔpH-dependent nonphotochemical quenching of chlorophyll fluorescence in spinach chloroplsts. *Biochim. Biophys. Acta* 1183: 339–344.

Pogson, B.J., Niyogi, K.K., Björkman, O. and DellaPenna, D. (1998) Altered xanthophyll compositions adversely affect chlorophyll accumulation and nonphotochemical quenching in *Arabidopsis* mutants. *Proc. Natl. Acad. Sci. USA* 95: 13324–13329.

Ruban, A.V., Young, A.J. and Horton, P. (1993) Induction of nonphotochemical energy dissipation and absorbance changes in leaves. *Plant Physiol.* 102: 741–750.

Schreiber, U., Klughammer, C. and Neubauer, C. (1988) Measuring P700 absorbance changes around 830 nm with a new type of pulse modulation system. *Z. Naturforsch.* 43C: 686–698.

Schreiber, U. and Neubauer, C. (1987) The polyphasic rise of chlorophyll

Downloaded from https://academic.oup.com/pcp/article/40/11/1134/1880967 by U.S. Department of Justice user on 16 August 2022

fluorescence upon onset of strong continuous illumination: II. Partial control by the photosystem II donor side and possible ways of interpretation. *Z. Naturforsch.* 42C: 1255–1264.

Zito, F., Finazzi, G., Delosme, R., Nitschke, W., Picot, D. and Wollman, F.-A. (1999) The Q_o site of cytochrome b_6f complexes controls the activation of the LHCII kinase. *EMBO J.* 18: 2961–2969.

(Received April 20, 1999; Accepted August 30, 1999)

Downloaded from https://academic.oup.com/pcp/article/40/11/1134/1880967 by U.S. Department of Justice user on 16 August 2022